Pergamon

Progress in Surface Science, Vol. 59, No. 1–4, pp. 255–264, 1998

Printed in Great Britain
0079-6816/98 $19.00

PII: S0079-6816(98)00051-3

GIANT STOP BANDS AND DEFECT MODES IN ONE-DIMENSIONAL WAVEGUIDE WITH DANGLING SIDE BRANCHES

B. DJAFARI ROUHANI[1], J. O. VASSEUR[1], A. AKJOUJ[1], L. DOBRZYNSKI[1], M. S. KUSHWAHA[2], P. A. DEYMIER[3] and J. ZEMMOURI[4]

[1]Laboratoire de Dynamique et Structures des Matériaux Moléculaires, URA CNRS 801, Université de Lille I, 59655 Villeneuve d'Ascq, France
[2]Instituto de Fisica, Universidad Autonoma de Puebla, Apdo Post. J48, Puebla 72570, Mexico
[3]Department of Materials Science and Engineering, University of Arizona, Tucson, U.S.A.
[4]Laboratoire de Spectroscopie Hertzienne, URA CNRS 249, Université de Lille I, 59655 Villeneuve d'Ascq, France

Abstract

We investigate both the photonic and electronic band structure of a comb-like waveguide geometry in which dangling side branches are grafted along an infinite one-dimensional waveguide. In a periodic (superlattice like) waveguide, we report the opening-up of stop bands which originate both from the periodicity of the system and the resonant states of the grafted branches (which play the role of resonators). Wide gaps (narrow bands) can be obtained by grafting several dangling side branches at every node. The stop bands still remain even for identical constituent materials. We also propose a tandem structure composed of two or several successive combs which differ by their physical characteristics that allows an ultrawideband filter. This behavior results from the superposition of the bandgaps in the successive structures. The presence of a defect branch in the comb can give rise to localized modes inside gaps. These states appear as very narrow peaks in the transmission spectrum and therefore may have useful applications in the frame of photonic bandgap materials or electronic band engineering of nanostructures.

1. Introduction

For the last ten years, numerous theoretical and experimental investigations have focused on the existence of gaps in the electromagnetic band structure of *photonic crystals*, i.e., artificial structures exhibiting a spatially dependent dielectric constant. Various 1D, 2D and 3D structures of periodic photonic crystals were studied [1]. Gaps were also observed in slightly disordered [2,3] as well as in quasiperiodic [4] 2D photonic crystals. In these forbidden bands, electromagnetic modes, spontaneous emission and zero-point fluctuations are all absent [5]. These properties become more pronounced when the gap is made large. Some studies have also addressed the problem of the emergence of localized states in the photonic band gaps by introducing defects in the periodic dielectric structure, for instance by removing or adding some inclusions [1,6-8] or by changing the characteristics (material or diameter) of several inclusions [9]. These properties were also started to be investigated

in quasi-one-dimensional photonic crystals [1,10]. Photonic crystals possessing localized modes in the forbidden bands should have applications in optical devices such as selective frequency filters or very efficient waveguides.

In two previous papers [11,12], we proposed a model of a quasi-one-dimensional photonic crystal exhibiting very narrow pass bands separated by large forbidden bands. This system is composed of an infinite one-dimensional waveguide (*the backbone*) along which stars of N' finite side branches are grafted at N equidistant sites, N and N' being integers (Fig.1). The backbone and the side branches are assumed to be infinitesimally thin wires. This *star wave guide* is described by two structural and two compositional parameters, namely the periodicity d_1, the length d_2 of each side branch, and the relative dielectric permittivity ε_i of each medium, with i=1 for the backbone and i=2 for the side branches.

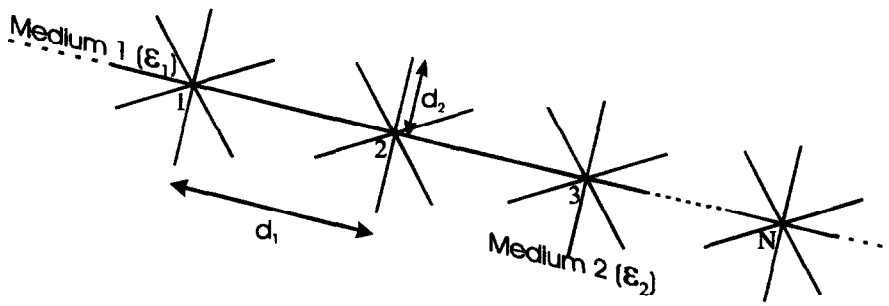

Fig. 1 : Periodic wave guide with N stars of N' (N'=6, here) grafted branches.

The stop bands originate both from the periodicity of the system and the resonant states of the grafted branches which play the role of resonators. Wide gaps/narrow bands can be obtained by an appropriate choice of the parameters, in particular the ratio between the two characteristic lengths d_1 and d_2, but more especially by grafting several dangling side branches at every node. Let us stress that, unlike in usual photonic crystals [1], relatively large gaps still remain for homogeneous systems where the side branches and the backbone are constituted of the same material. The main features of our model will be briefly presented in § 2, followed by two new results. First, we show that very large gaps in some specific frequency ranges can be realized by considering a tandem structure composed of two or several successive star waveguides which differ by their physical characteristics. Then, we investigate the existence of localized modes inside gaps when a defect branch of different length is inserted in the star waveguide.

These results obtained for electromagnetic waves will be transposed in § 3 to electronic excitations in the frame of an effective mass model [13]. The motivation behind this work is to demonstrate the

control over the widths of the pass bands and hence the gaps. Let us emphasize several investigations of the electronic transport in 1D structures with a wide variety of geometries. One can mention the quantum conductance in 1D mesoscopic rings [14], the transmission zeros and poles in quantum waveguides [15], the transport properties of waveguide like T-shaped semiconductors structures exhibiting transistor action based on quantum interference [16], the effect of short-range irregularities on transmission in coupled quantum wires [17], the size effect on conductance in ballistic quantum wires [18] and the experimental observation of quantum corrections to the resistance in 1D gold wires with periodically spaced dangling side branches [19].

2. Giant Photonic Stop Bands and Defect Modes

The passing and stop bands of the star waveguide depicted in Fig. 1 can be displayed in the dispersion relation for an infinite number of sites ($N \to \infty$) or in the transmission coefficient T through the waveguide when the side branches are grafted at a finite number N of nodes. Both the dispersion relation and the transmission factor T were obtained in a closed form by using the interface response theory [11,20]. They are given as :

$$\cos(kd_1) = C_1 + \frac{N'}{2}.\frac{F_2}{F_1}.\frac{S_1 C_2}{S_2} \tag{2.1}$$

or

$$\cos(kd_1) = C_1 + \frac{N'}{2}.\frac{F_2}{F_1}.\frac{S_1 S_2}{C_2} \tag{2.2}$$

and

$$T = \left| \frac{2S_1\left(t^2 - 1\right)t^N}{\left[1 - t\left(C_1 - S_1\right)\right]^2 - t^{2N}\left[t - \left(C_1 - S_1\right)\right]^2} \right|^2 \tag{2.3}$$

where k is the modulus of the wave vector for propagation of electromagnetic waves in the interior of the star waveguide and $t = \exp(ikd_1)$. In equations (2.1), (2.2) and (2.3), the quantities C_i, S_i and F_i (i=1,2) are defined as $C_i = \cosh(\alpha_i d_i)$, $S_i = \sinh(\alpha_i d_i)$ and $F_i = \alpha_i$ with $\alpha_i = j\frac{\omega}{c}\sqrt{\varepsilon_i}$ where ω is the frequency, c the speed of light in vacuum and $j = \sqrt{-1}$.

The dispersion relations (2.1) and (2.2) were obtained for two different choices of the boundary conditions, namely, the vanishing of either the electric field (E=0) or the magnetic field (H=0) at the free extremities of the side branches. The wavevector k is then defined by either (2.1) or (2.2).

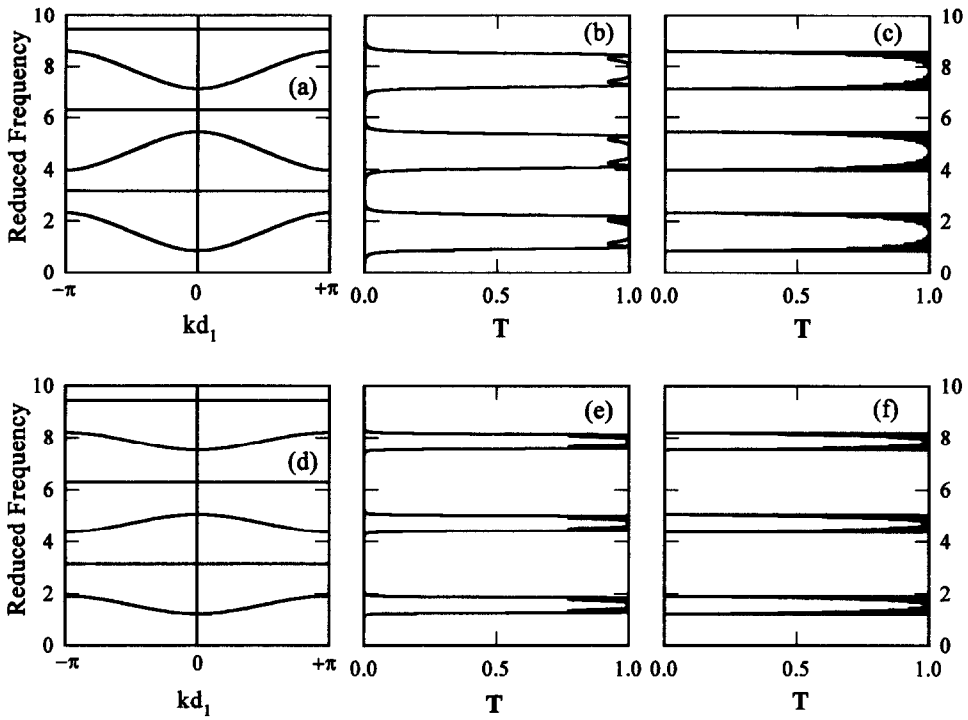

Fig. 2: Top panel: (a) Dispersion curves (reduced frequency $\Omega = \omega d_1 \sqrt{\varepsilon_1}/c$ versus the dimensionless wave vector kd_1) for the one-dimensional structure depicted in Fig. 1, with N→ ∞, N'=1 and the boundary condition E=0. (b) and (c) Transmission coefficients through the same structure with the side branches grafted respectively at N=5 and N=10 nodes. Bottom panel: Same as in top panel, but for N'=4 side branches grafted at every node.

In Fig. 2, we present the band structures and transmission coefficients for star waveguides composed of identical constituents, i.e., $\varepsilon_1 = \varepsilon_2$, with the same characteristic lengths $d_1 = d_2$ and the boundary condition E=0. The top and bottom panels respectively describe the situations where the number of grafted side branches at every node is N'=1 and N'=4. Figure 2(a) shows the sixth lowest dispersion curves of the photonic band structure for N→ ∞ and N'=1. In this periodic system, one can notice the presence of pass bands separated by gaps and in particular the existence of a cutoff frequency, i.e., a forbidden band which commences at zero frequency. The flat bands at reduced frequencies equal to π, 2π, 3π,... correspond to localized modes inside each resonator. These modes do not penetrate into the backbone. In Fig. 2(b), we have plotted the variations of the transmission coefficient T versus the reduced frequency for a finite number of stars, namely N=5. Despite the finite number of resonators, one can notice that T approaches zero in regions corresponding to the observed

gaps in the electromagnetic band structure of Fig. 2(a). The flat bands in Fig. 2(a), associated with localized modes inside the resonators, do not contribute to the transmission. Fig. 2(c) shows that increasing the number N of nodes to 10 does not modify significantly the edges of the forbidden bands. The bottom panel of Fig. 2 contains similar results to those of the top panel when several (N'=4) side branches are grafted at every node. This panel illustrates the narrowing (widening) of the pass bands (forbidden bands) when increasing N'.

A detailed analysis of the photonic band structure in our model with the boundary condition H=0 at the free extremities of the side branches is presented in our recent works [11,12]. There, we have also discussed other possibilities of making some of the pass bands narrow by an appropriate choice of the characteristic lengths d_1 and d_2. A simple experimental confirmation of our theoretical predictions was also achieved by measuring the transmission coefficient through star waveguide structures constituted by coaxial cables. The typical lengths d_1 or d_2 in these experiments is of the order of one meter, therefore the observed gaps fall in the frequency range of a few to 500 MHz. However, the physical behavior predicted in our model should remain valid in other frequency domains of the electromagnetic spectrum, as recent manufacturing techniques permit the fabrication of extremely thin wires [21-23].

We propose, in this paper, another way of making an ultrawideband filter in some frequency domains. This consists in a tandem structure composed of a series of two or more combs which differ by their characteristic lengths, material parameters or boundary conditions. Indeed, the transmission coefficient through the tandem can be suppressed by taking advantage of the superposition of the gaps in individual combs. Two examples are depicted in Figs. 3, for tandem structures containing two different combs. One can notice that the transmission through the tandem (bottom panel) is significantly depressed in the gaps of individual combs (top and middle panels). From a technical point of view, one may expect that the realization of the tandem structure would be easier than grafting several side branches at every node of a comb.

Finally, we address in this section the problem of the existence of localized modes in the forbidden bands of the photonic structure resulting from the presence of a defect side branch inside a comb. For the sake of briefness, we concentrate on the case of a defect branch differing by its length d_3 from the normal branches of length d_2. Fig. 4 gives the frequencies of the localized modes as a function of d_3 when a defect is introduced into an infinite comb. The hatched areas correspond to the bulk bands of the perfect comb. The localized modes emerge from the bulk bands, decrease in frequency by increasing d_3 and finally merge into a lower bulk band. At each frequency, there is a periodical repetition of the localized state as a function of d_3.

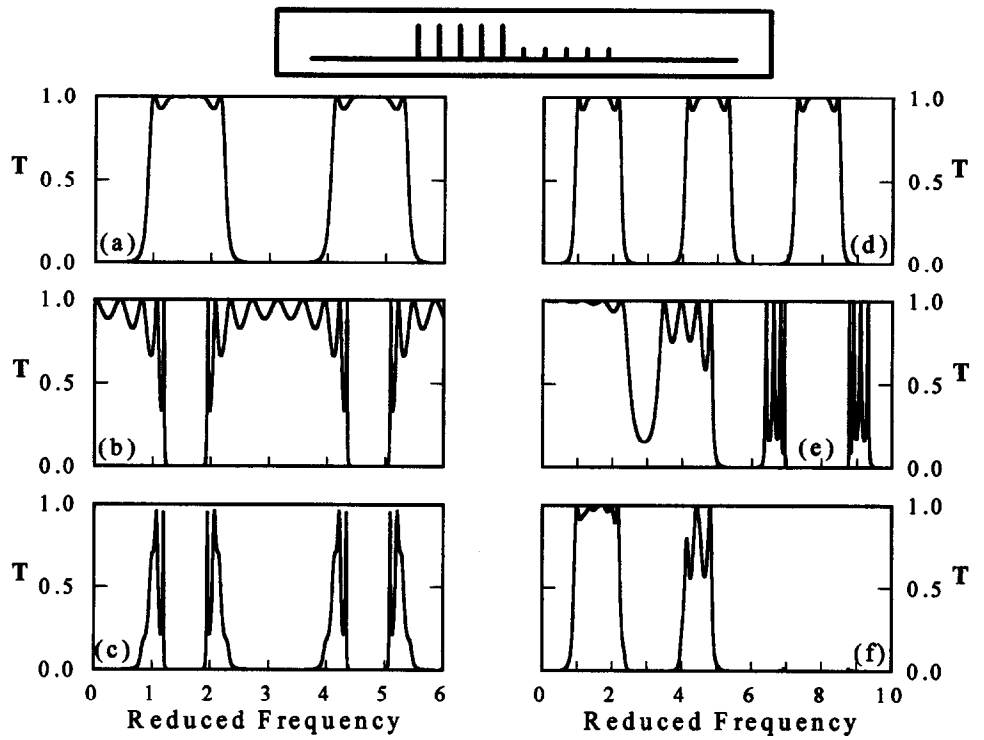

Fig. 3: Transmission coefficients through individual combs (top and middle panels) and through the tandem structure (lower panel). In the left panel, the parameters of the individual combs are $\varepsilon_1=\varepsilon_2$, $d_1=d_2$, N=5, N'=1 and the combs differ by their boundary condition: E=0 in (a) and H=0 in (b). In the right panel, the characteristic length d_2 of the second comb is also changed to $d_2=0.2\ d_1$.

The transmission coefficient is also affected by the presence of a defect inside the comb and, in particular, exhibits narrow peaks associated with the localized modes. Figure 5 gives a comparison of the transmission coefficients for two combs respectively with and without defect. In the frequency range displayed in this figure, there are five peaks associated with the localized states, those falling in the middle of a gap being much narrower than those situated in the vicinity of a band edge. The transmission inside a bulk band can also be significantly affected by the presence of a defect. For instance, in our example, T is totally depressed inside the second bulk band (Figs. 5(b) and 5(c)). Another point to notice in Fig. 5 is the influence of the location of the defect site on the transmission coefficient and in particular on the intensities of the peaks associated with the localized modes. Experimental proofs of the above results are in progress and will be published elsewhere.

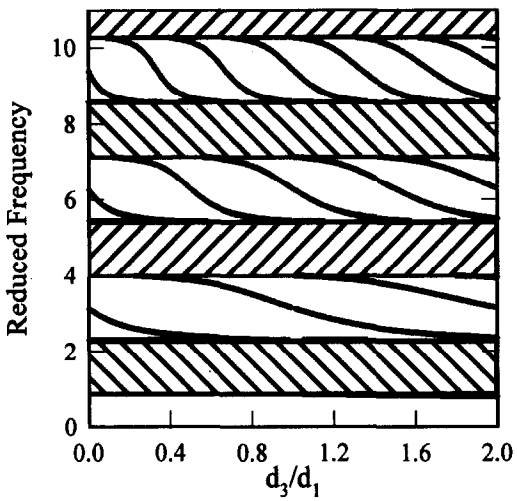

Fig. 4: Frequencies of the localized modes associated with a defect side branch of length d_3 in an infinite comb. The other parameters are $\varepsilon_1 = \varepsilon_2 = \varepsilon_3, d_1 = d_2, N' = 1$ and the boundary condition is E=0.

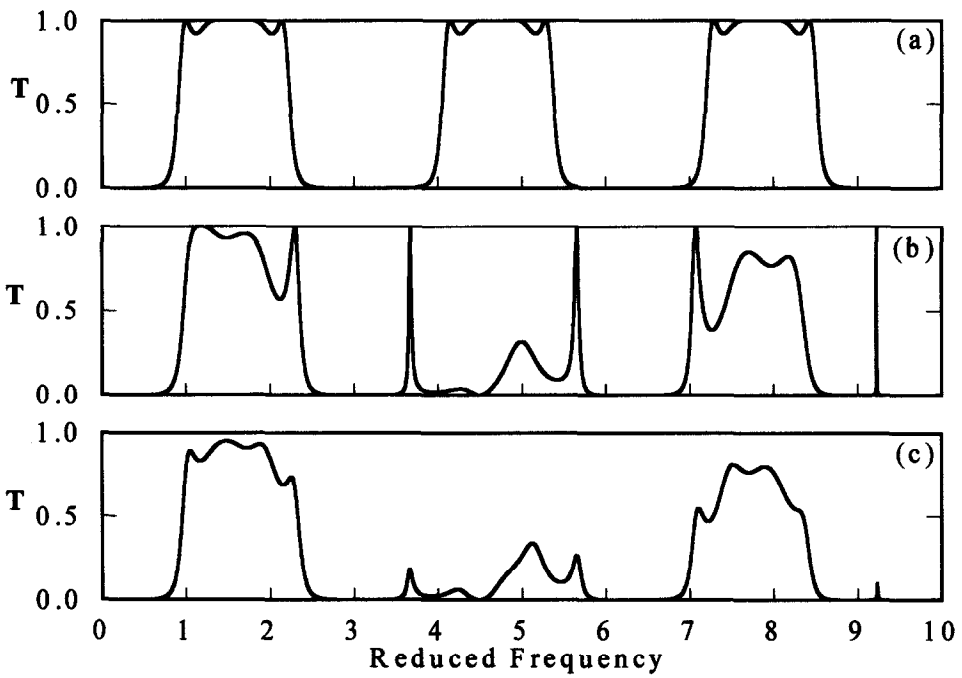

Fig. 5: Transmission coefficients for a perfect and a defective combs containing N=5 nodes. (a) The comb is without defect. (b) The comb contains one defect side branch of length $d_3=0.7d_1$ located at the middle node. (c) The defect is located on the second (or on the fourth) node. The other parameters are $\varepsilon_1 = \varepsilon_2 = \varepsilon_3, d_1 = d_2, N' = 1$ and the boundary condition is E=0.

3. Giant Electronic Stop Bands and Defect Modes

The above formalism can also be used to investigate the band structure of a *comb-like* electronic waveguide provided each material is described in the frame of an effective mass model. The analytic expressions derived for the photonic structure can be transposed to the electronic excitations provided the quantities α_i and F_i are defined as $\alpha_i = \frac{1}{\hbar}\sqrt{2m_i(V_i - E)}$ and $F_i = \frac{\hbar^2}{2m_i}\alpha_i$, where $\hbar, m_i, V_i$ refer, respectively, to the reduced Planck constant, the effective mass and a constant potential in medium i. In our model, the potential V_1 in the backbone is assumed to be lower than the potential V_2 in the side branches and the energy E defined as $E = \frac{\hbar^2 k^2}{2m_i} + V_i$ (where k is a one-dimensional wavevector) should be higher than the potential V_1 [13]. With these notations, the electronic band structure and the transmission factor are respectively given by (2.1) and (2.3), where the usual boundary conditions (i.e., the continuity of the wavefunctions and their first derivatives divided by the respective effective masses) has been employed.

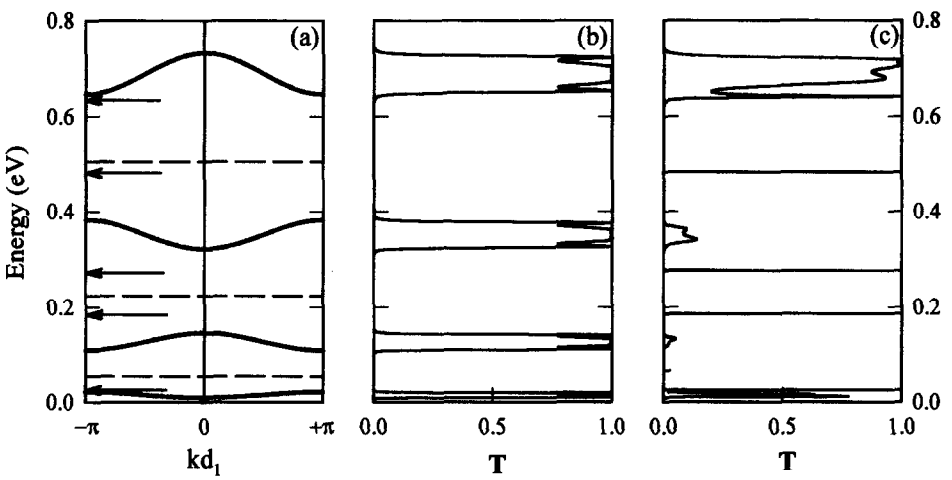

Fig. 6: (a) Dispersion curves of the electronic states in a star waveguide made of GaAs, with $N \to \infty$, $d_1 = d_2 = 10$ nm and $N' = 4$. The arrows indicate the energies of localized modes associated with a star made of N' defect side branches of length $d_3 = 7.0$ nm. The dashed lines are flat bands which do not contribute to the transmission. (b) and (c) Transmission coefficients through the same structure with the side branches grafted at N=5 nodes, respectively without star defect and with one star defect located on the middle node.

Considering the material media GaAs for the backbone and GaAs or Ga_{1-x} Al_x As for the side branches, we have investigated [13] the electronic band structure of the comblike waveguide. We have shown in particular the narrowing (widening) of the bands (gaps) by increasing the number N' of grafted side branches at every node. In Fig. 6, we present an example of the dispersion curves and transmission coefficient for a star waveguide with GaAs as the only constituent and we show the existence of localized states when the length of the side branches at one node is changed from d_2 to d_3. In the energy range depicted in Fig. 6, there are five localized modes associated with this defect; the corresponding peaks in the transmission being narrower when falling in the middle of a gap.

4. Conclusions

In this paper, we have investigated the photonic or electronic band structure of a quasi-one dimensional periodic system with a comblike structure which can exhibit very large forbidden bands. Localized states associated with defects in the comb were observed. These defect modes appear as narrow peaks of strong amplitude in the transmission spectrum. The manufacturing of such waveguides could be very useful in making, for instance, filtering or multiplexing devices, more particularly in integrated structures working at optical frequencies. Comb-like nanostructures could also have potential applications in modern semiconductor technology. The generalization of our one-dimensional model to the case of a 2 or 3-dimensional network of connected wires is also possible. Finally, we would mention our recent application of this theory to the study of acoustic spectral gaps and discrete transmission in slender tubes [24].

References

1. See for example, J.D. Joannopoulos, R.D. Meade and J.N. Winn, *Photonic Crystals,* Princeton University Press, Princeton (1995); *Photonic Band Gaps and Localization*, C.M. Soukoulis (Ed.), Plenum, New York (1993); *Photonic Band Gap Materials*, C.M. Soukoulis (Ed.), Kluwer, Dordrecht (1996).
2. M.M. Sigalas, C.M. Soukoulis, C.T. Chan and D. Turner : Phys. Rev. B **53**, 8340 (1996).
3. H. Li, B. Cheng and D. Zhang, Phys. Rev. B **56**, 10734 (1997).
4. Y.S. Chan, C.T. Chan and Z.Y. Liu, Phys. Rev. Lett. **80**, 956 (1998).
5. E. Yablonovitch, J. Opt. Soc. Am. B **10**, 283 (1993).
6. M. Sigalas, C.M. Soukoulis, E.N. Economou, C.T. Chan and K.M. Ho, Phys. Rev. B **48**, 14121 (1993).

7. E. Yablonovitch, T.J. Gmitter, R.D. Meade, A.M. Rappe, K.D. Brommer and J.D. Joannopoulos, Phys. Rev. Lett. **67**, 3380 (1991).
8. A. Mekis, J.C. Chen, I. Kurland, S. Fan, P.R. Villeneuve and J.D. Joannopoulos, Phys. Rev. Lett. **77**, 3787 (1996) .
9. K. Sakoda and H. Shiroma, Phys. Rev. B **56**, 4830 (1997).
10. S. Foresi, P.R. Villeneuve, J. Ferrera, E.R. Thoen, G. Steinmeyer, S. Fan, J.D. Joannopoulos, L.C. Kimerling, Henry I. Smith and E.P. Ippen, Nature **390**, 143 (1997).
11. J.O. Vasseur, P.A. Deymier, L. Dobrzynski, B. Djafari Rouhani and A. Akjouj, Phys. Rev. B **55**, 10434 (1997).
12. L. Dobrzynski, A. Akjouj, B. Djafari Rouhani, J.O. Vasseur and J. Zemmouri, Phys. Rev. B **57**, R9388 (1998).
13. A. Akjouj, L. Dobrzynski, B. Djafari Rouhani, J.O. Vasseur and M.S. Kushwaha, Europhys. Lett. **41**, 321 (1998).
14. D. Takai and K. Ohta, Phys. Rev. B **51**, 11132 (1995).
15. Z. Shao, W. Porod and C.S. Lent, Phys. Rev. B **49**, 7453 (1994).
16. F. Sols, M. Macucci, U. Ravaioli and K. Hess, J. Appl. Phys. **66**, 3892 (1989).
17. Ch. Kunze, Phys. Rev. B **48**, 14338 (1993).
18. T. Itoh, N. Sano and A. Yoshi, Phys.Rev. B **45**, 14131 (1992).
19. M.E. Gerhenson, P.M. Echternach, A.G. Mikhalchuk, H.M. Bozler, A.L. Bogdanov and B. Nilson, Phys. Rev. B **51**, 10256 (1995).
20. L. Dobrzynski, Surf. Sci. **180**, 489 (1987)
21. A. Blondel, J.P. Meier, B. Boudin and J.-Ph. Ansermet, Appl. Phys. Lett. **65**, 3019 (1994).
22. J. de la Figuera, M.A. Huerta-Garnica, J.E. Prioto, C. Ocal and P. Miranda, Appl. Phys. Lett. **66**, 1006 (1995).
23. W.Z. Li, S. S. Xie, L. X. Qian, B.H. Chang, B.S. Zou, W.Y. Zhou, R.A. Zhao and G. Wang, Science **274**, 1701 (1996).
24. M.S. Kushwaha, A. Akjouj, B. Djafari-Rouhani, L. Dobrzynski and J.O. Vasseur, Solid State Comm. **106**, 659 (1998).